Jurnal Rekayasa Kimia dan Lingkungan
(Journal of Chemical Engineering and Environment)
Volume 17, Number 2, Page 152 – 162, July - December, 2022
ISSN 1412-5064, e-ISSN 2356-1661
https://doi.org/10.23955/rkl.v17i2.26692

# Characterization and Application of HCl-Activated LTA Zeolite from Lampung Natural Zeolite (LNZ) for Bioethanol Purification

**Simparmin Br. Ginting[1*], Ulfa Islamia[1], Darmansyah[2], Herry Wardono[3]**

[1] Departement of Chemical Engineering, Faculty of Engineering, University of Lampung,
Jl. Prof. Sumantri Brojonegoro No.1 Bandar Lampung, 35145
[2] Graduate School of Chemical Engineering, Faculty of Engineering, University of Lampung,
Jl. Prof. Sumantri Brojonegoro No.1 Bandar Lampung, 35145
*E-mail: simparmin.ginting@eng.unila.ac.id

Article History
Received: 1 July 2022; Received in Revision: 7 November 2022; Accepted: 20 November 2022

**Abstract**

Lynde Type-A (LTA) zeolite as being molecular sieve and hydrophilic zeolite is used to dehydrate water in the purification of bioethanol. LTA zeolite from LNZ has a small surface area of 29,62 $m^2/g$. LTA Zeolite could be activated with HCl to increase the surface area as well as its performance. The activation of LTA zeolite was carried through in a closed erlenmeyer with various HCl concentration: 10% w/w, 15 % w/w, and 20% w/w and the ratio acid/LTA zeolite was 10 ml: 1 gram. The performance of LTA zeolite activated by HCl concentrations was examined in the process of bioethanol purification using extractive batch. The XRD analysis showed that the structure of LTA zeolite activated does not change despite the process of activation, and the highest percentage of crystallinity was obtained at 68.25% wt by concentration of HCl at 20 % w/w. The result of FTIR analysis, all LTA zeolites after activated by HCl showed double rings as the main characteristic of LTA Zeolite, and formed open pores. The result of XRF analysis showed that the highest of impurity removal was of Mg, P, K, Ca, and Fe while the highest decreasing ratio of Si/Al was in the LTA zeolite activated by HCl 20% w/w. The result of BET analysis showed the largest surface area at 45.67 $m^2/g$ obtained by adding 10% w/w of HCl activator, which was 45.67 $m^2/g$, and the size of zeolite's pore volume was 0.027 cc/g. The results of SEM analysis showed that LTA Zeolite crystals have cubical morphology and the higher concentration of HCl, the lower amorphous shape in zeolite. LTA zeolite being activated by HCl concentration 20% w/w, obtained the highest purity of bioethanol by 99.74 % v/v. The water adsorption isotherm model of LTA Zeolite activated by concentration of HCl at 20 % w/w follows the Langmuir isotherm model with a correlation coefficient ($R^2$) = 0.9870, adsorption capacity (qm) = 83.33 mg water/g adsorbent and zeolite adsorption intensity (Ka) = 0.01. The water adsorption kinetic model follows the criteria of the kinetic pseudo second order with a reaction rate value of 0.4360 g/(min-mg) and qe = 0.2695 mg water/g adsorbent.

Keywords: Zeolite Lynde Type-A (LTA), fuel grade ethanol, molecular sieve, activation of zeolite lynde type-A (LTA) with HCl, natural lampung zeolite

## 1. Introduction

Bioethanol purification can be carried out through a dehydration-adsorptive process based on the molecular sieve principle. Purification using molecular sieve LTA zeolite is relatively inexpensive and simple because it can be used repeatedly and uses low energy, has high dehydration ability, and is environmentally friendly (Ranjbar, 2012)

In previous studies, LTA zeolite was made from Lampung Natural Zeolite (LNZ, also known as ZAL) raw materials, but it was still not optimal due to the low level of purity of the raw materials used, namely: LNZ which still contains a lot of impurities such as $Na^+$, $K^+$, $Fe^{3+}$, $Mg^{2+}$, and $Ca^{2+}$ (Wardono et al., 2018) This deficiency makes the LTA zeolite produced from LNZ needs to be activated to remove impurities and produce better characteristics. LTA zeolite activation process can be done by physical and chemical methods. Chemical activation can be done with the addition of acid which results in the exchange of cations with $H^+$ to remove metal impurities so that the zeolite becomes more porous and the surface of the contact area becomes larger (Wang et al., 2012)

The latest research on this topic is to determinate the ratio of the HCl solution volume on zeolite as well as the concentration given were obtained from Panitchakarn et al., 2014 who have conducted a research on the effect of HCl acid activation (10 - 30%w/w) on

Coal fly ash as a source of silica-alumina in the synthesis of LTA zeolite. From the results of the study, it was found that HCl at a concentration of 20% w/w, with a ratio of L/S ml acid/gram Coal fly ash = 20 ml/gram is the most effective for removing impurities in CBA (Coal Bottom Ash) so as to increase the percent crystallinity of the product by 85% wt. Based on the results of XRD and BET analysis, the product obtained from HCl-activated CFA had the best purity of 87% wt. (Ferella et al., 2019) have investigated the effect of HCl acid activation on a spent FCC (SFCC) catalyst (consisting of zeolite Y attached to the active matrix of silica-alumina-clay) as a raw material in the synthesis of zeolite Y. The activation process was carried out at a ratio of HCl/SFCC acid solution (L/S) = 10:1, with an HCl concentration of 0.8-1.6 mol/liter. From the BET results, activated SFCC has a surface area of 197.1 $m^2$/gram, a total pore volume of 0.1987 cc/gram, while SFCC without activation has a specific surface area of 91.9 $m^2$/gram, a pore volume of 0.116 cc/gram (Panitchakarn et al., 2014). It can be concluded that the addition of HCl acid activators in zeolite can remove metal impurities that affect the contact surface area and total pore volume of zeolite samples.

Thus, this research refers to the research conducted by Ginting et al., 2019 has been synthesized the LTA zeolite from Lampung Natural Zeolite using the step change temperature of hydrothermal method with variations of $SiO_2/Al_2O_3$ for use in ethanol dehydration", with the best results shown in LTA zeolite with a $SiO_2/Al_2O_3$ ratio of 1.8 mol/mol, which has a contact surface area of 15.70 $m^2$/gram, a pore volume of 0.0483 cc/gram and has a percent crystallinity level of LTA zeolite of 71.39% wt. That research didn't activate the LTA zeolite (Ginting et al., 2019). In order to get higher result in this paper having activation of LTA zeolite from LN zeolite. The activation was using HCl with variations by adding the concentration of HCl activators in the LTA zeolite of: 10% w/w, 15% w/w, and 20% w/w with a ratio of HCl/LTA zeolite activators solution = 10 ml/gram in order to increase the characteristic of LTA, specifically the surface area, so that there is an increase in the ability to absorb water from a water-ethanol mixture. The activation process for LTA zeolite is able to remove metal impurities that cover the pores and channels of the zeolite which will increase the surface area and pore volume of the LTA zeolite thereby increasing the water adsorption ability of ethanol-water.

## 2. Methodology

### 2.1. Materials

The research materials used in this study were NaOH p.a. Merck, Merck HCl 37%v, aquadest, Merck anhydrous aluminum oxide 99% v. Those chemicals were purchased from Merck KGaA, EMD Millipore Corporation, USA. Technical ethanol 70% v and 96% v, Whatman filter paper no.40, diameter 125 mm, aluminum foil and LNZ from CV. Minatama, Lampung, Indonesia.

### 2.2. Synthesis of the Activated LTA Zeolite

The manufacture of LTA zeolite refers to a research from Ginting et al. (2019). Grinding and sieving LNZ into 200 mesh; preparation of aluminasilicate synthesis solution and LNZ was mixed at a temperature of 60$^o$C, atmospheric pressure and stirred for 1 hour in a closed erlemeyer with the molar composition of the reactant mixture: $SiO_2/Al_2O_3$: 1.80, $Na_2O/Al_2O_3$: 3.16, $H_2O/Al_2O_3$: 128 (Mirfendereski & Mohammadi, 2016). Next step was crystallizing the precursor LNZ-aluminasilicate solution into LTA zeolite by applying the step change of temperature hydrothermal method for the precursor of LTA zeolite solution in the water-bath (Hui and Chao, 2006; Sharma et al., 2015). Dried LTA zeolite and activated LTA zeolite with HCl. The ratio of the HCl/LTA zeolite solution used was 10 ml: 1 gram. The preparation of the activation at a temperature of 80$^o$C, atmospheric pressure and stirred for 1 hour in a closed erlemeyer with various concentrations of 10% w/w, 15% w/w, and 20% w/w. The ratio of the HCl/LTA zeolite solution used was 10 ml : 1 gram. While it was being activated, the temperature need to set and control at 80$^o$C using bekker glass. The last step, dried all the activated LTA zeolites.

### 2.3. Adsorption Experiment

Performance test of synthesized LTA zeolite before and after activation of HCl concentrations was at 10% w/w, 15% w/w, and 20% w/w in ethanol-water adsorptive dehydration which was carried out in batches with several steps, namely the first, testing the water adsorption by the sample of the LTA zeolite synthesized product that has been mentioned as much as 2 grams with 10 ml technical ethanol (95% v/v purity) for 1 hour. Second, the best yield of LTA zeolite (at the highest ethanol purity) from the first step was immersed until it reached equilibrium time

with technical ethanol at 95% v/v. Finally, variations in the concentration of ethanol content (70, 75, 85, and 95% v/v) with LTA zeolite from the best ethanol-water adsorption results (at the highest ethanol purity) was used to determine the equilibrium concentration. These steps were to determine: adsorption ability, equilibrium characteristics of adsorption isotherms, adsorption kinetics, and adsorption capacity.

### 2.4. Characterization Analysis

The analysis/characterization stages include: Functional group analysis was carried out and recorded using IRAffinity-1S FTIR spectrometer, Composition content analysis was carried out and recorded using X-Ray Fluoresence analysis, Brunauer Emmett Teller analysis on LTA zeolites (non-activator, 10% w/w, 15% w/w, and 20 % w/w HCl content), The morphology of HCl-activated LTA zeolite was examined on a Scanning Electron Microscope analysis (JSM-636OLA), and analysis with a calibrated hydrometer and pycnometer to determine the levels of bioethanol contained during the adsorption test.

## 3. Results and Discussion

### 3.1. XRF Analysis Result

The result of XRF analysis showed the metal impurities in zeolite decrease more and more along with the increase in the concentration of the HCl activators which is shown in Table 1. On decreasing levels where the metal impurities are in the form of alkaline and alkaline earth groups such as K, Ca, Ba, and Sr, deionization occurs, which is the exchange of cations - alkaline and alkaline earth cations with $Cl^-$ ions into a salt solution which will dissolve with water after neutralizing the pH and cause a decrease in the level of metal impurities in the zeolite. In addition, metal impurities in the form of heavy metal groups such as Eu, Ir, Y, Fe, Zr, Ga, Mn, Zn and Ce are also soluble in HCl acid. Meanwhile, the $Cl^-$ ion component increased at 10% w/w and 15% w/w in HCl levels, and decreased at 20% w/w in HCl levels. The content of $Cl^-$ ions that still persists after the activation process in the zeolite is due to the influence of the formation of Bronsted and Lewis acid sites when heating is carried out less than 299.85◦C (Cakicioglu-Ozkan & Ulku, 2005), which causes $Cl^-$ ions to bind strongly to the zeolite and fill the volume of zeolite pores so that it is able to reduce the size of the zeolite pores. In this study, heating was carried out only at a temperature of 105 ◦C causing the $Cl^-$ ions to take a very long time during the washing process to be removed (Jankowska et al., 1991). Meanwhile, at the time of activation with a concentration of 20% w/w, the $Cl^-$ ion content can be reduced and produce the lowest $Cl^-$ content rate due to the large concentration of activators so that it is able to bind alkali metals, alkaline earth and dissolve more heavy metals, thus forming salt bond, when reacting with HCl so that it is easier to purify than at 10% w/w and 15% w/w activation levels where the $Cl^-$ ions are reduced more. Another possibility of an increase in metal impurities after activation is probably because the washing process and the metal destruction process used aqua dest instead of aqua bidest. It is known that there are still many dissolved metals in aqua dest (Heraldy E, et al, 2003). Where in Table 1, there is a metal content that decreases the most after activation at 20% w/w of HCl concentration before the activation is carried out, namely Mg metal from 1.229% to 0.311%; metal P from 4.624% to 1.07%; metal K from 6.157% to 1.07%; metal Ca from 8.706% to 1.909%; and Fe metal from 4.455% to 0.723%.

**Table 1.** Element content of Nonactivated and Activated HCl Zeolite A.

| Element | Total Element Content of Zeolite at Variations HCl Concentrate (%w/w) | | | |
|---|---|---|---|---|
| | 0 (%) | 10 (%) | 15 (%) | 20 (%) |
| Mg | 1.229 | 3.643 | 3.039 | 0.311 |
| Al | 32.903 | 31.493 | 38.65 | 44.117 |
| Si | 39.959 | 44.394 | 51.842 | 50.408 |
| P | 4.624 | 9.678 | 1.124 | 1.070 |
| Cl | 0.049 | 0.053 | 0.086 | 0.010 |
| K | 6.157 | 1.774 | 1.043 | 0.911 |
| Ca | 8.706 | 5.777 | 2.003 | 1.909 |
| Ti | 0.372 | 0.477 | 0.176 | 0.155 |
| Mn | 0.136 | 0.021 | 0.014 | 0.010 |
| Fe | 4.455 | 1.538 | 1.165 | 0.723 |
| Zn | 0.032 | 0.008 | 0.004 | 0.002 |
| Ga | 0.035 | 0.009 | 0.014 | 0.009 |
| Sr | 0.122 | 0.013 | 0.020 | 0.014 |
| Zr | 0.064 | 0.034 | 0.020 | 0.012 |
| Ag | 0.632 | 0.942 | 0.712 | 0.287 |
| Ba | 0.400 | 0.138 | 0.061 | 0.042 |
| Eu | 0.043 | 0 | 0.007 | 0 |
| Ir | 0.003 | 0 | 0 | 0 |
| Rb | 0.046 | 0 | 0 | 0 |
| Y | 0.010 | 0.006 | 0.008 | 0.002 |
| Ce | 0.021 | 0 | 0 | 0 |
| Br | 0 | 0 | 0.006 | 0.002 |

Meanwhile, the main component of LTA zeolite in the form of silica (Si) and alumina (Al) can be seen through the value of the Si/Al molar ratio in the zeolite. Changes in the Si/Al molar ratio of a zeolite material can affect the properties of the material. The molar value of Si/Al zeolite shows the large content of negative charges in the zeolite. The greater the amount of Alumina in the zeolite framework that can replace Silica, the smaller the Si/Al molar value and the greater the negative charge of the zeolite (Neolaka et al., 2022). This happened in the activation of LTA zeolite with 20% w/w HCl content where most of the impurities were removed during activation compared to 10% w/w and 15% w/w of activator levels.

The decrease in the Si/Al ratio will increase the adsorption capacity and selectivity of the zeolite towards polar molecules such as water vapor(Bulut et al., 2008). Meanwhile, the activator concentration of 10% w/w showed an increase in the Si/Al ratio, because HCl was more active in breaking alumina from the zeolite framework and causing dealumination compared to removing impurities. Thus, the decrease in the Al content in the zeolite causes the Si/Al mol ratio to increase. The following is the reaction for the release of Al from the zeolite framework by HCl solvent (dealumination).

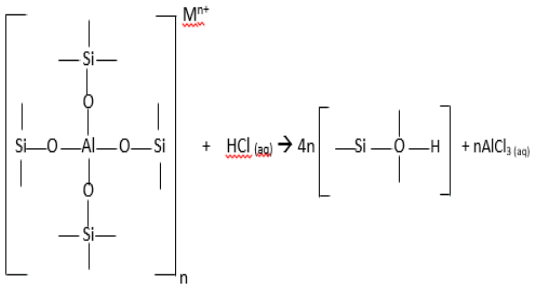


**Figure 1.** Al release reaction in Zeolite Framework (Pardoyo, et al, 2009).

**Table 2.** The Si/Al Content Ratio of Zeolite A.

| Sample | Total Si/Al Ratio (mol/mol) |
|---|---|
| Zeolite A 0% w/w | 1.21 |
| Zeolite A 10% w/w | 1.41 |
| Zeolite A 15% w/w | 1.34 |
| Zeolite A 20% w/w | 1.14 |

While at an activator concentration of 15% w/w, HCl was more active in binding alkaline and alkaline earth impurities on the surface of the zeolite (decationization) and dissolving heavy metals and impurities more than the previous activator concentration but did not cause dealumination and Si level increase, so the Si/Al ratio increased prior to the activation. (Triantafillidis & Evmiridis, 2000). Table 2 shows the Si/Al molar ratio in LTA zeolites.

### 3.2. XRD Analysis

The percent crystallinity value from the result of XRD analysis based on the calculations of Rayalu et al., (2005) shown in Table 3.

**Table 3.** Percent Crystallinity of Zeolite A with Variation of Activator Concentration.

| Sample | Percent Crystallinity (% wt) |
|---|---|
| Zeolite A 0% w/w | 60.10 |
| Zeolite A 10% w/w | 48.00 |
| Zeolite A 15% w/w | 49.42 |
| Zeolite A 20% w/w | 68.25 |

From the XRD analysis of non-activated and activated LTA zeolite at levels of 10% w/w, 15% w/w and 20% w/w, it shows that the constituent minerals in the sample contain crystals of Calcium Alluminate Silicate, Quartz, Mullite, and zeolite A. The XRD results showed that at concentrations of 10% w/w and 15% w/w, very little zeolite A was formed and the XRD diffraction peak intensity of zeolite A was weak (lowest) compared to unactivated zeolite. While the results of XRD analysis of LTA zeolite at 20% w/w activation showed that the zeolite had more zeolite A crystals formed and the intensity of the XRD diffraction peak of zeolite A was stronger (higher) compared to the 3 LTA zeolites with the previous activator levels and also contained other minerals that are less in number such as Calcium Alluminate Silicate, Mullite, and Quartz crystals. It can be shown that the intensity is getting sharper in the post [°2Theta] area, namely 34.270 and 43.1657 (LTA Zeolite Standard ICDD No. 00-031-1261). The post [°2Theta] 34,270 consecutively has an interval intensity of 83.79; 95.85; 94.42 and 100.00%, whereas for the post [o2Theta] 43.1657 has an interval intensity of: 91.75; 98.44; 45.66; and 92.67%.

The decrease in the percent crystallization value of LTA zeolite after activation at concentrations of less than 20% w/w, which are: 10% w/w and 15% w/w due to the low level of HCl activators during activation, allows other crystals to form such as Calcium Alluminate crystals. Silicate, anorthite, and mullite so that it can reduce the number of crystals of zeolite A. This is because the formation produces more amorphous products than the crystal content. On activation with 10% w/w HCl a dealumination process occurs.

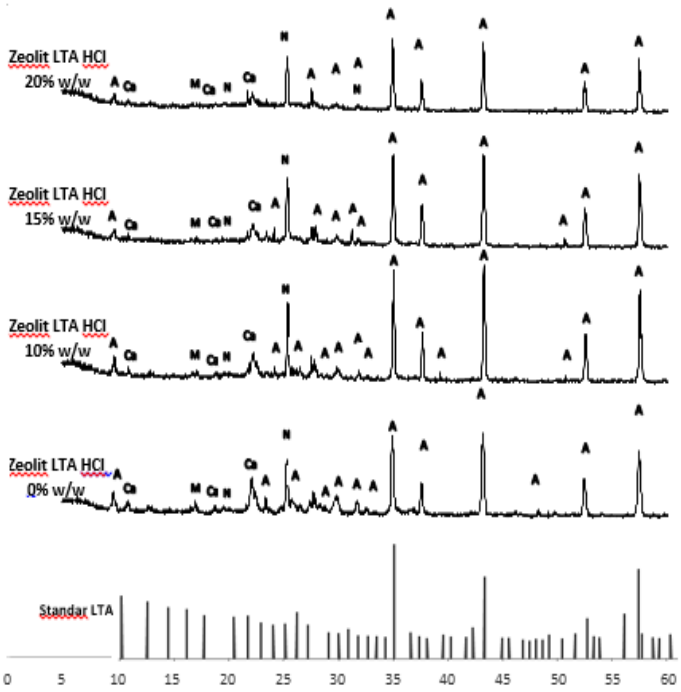


**Figure 2.** Results of XRD Analysis on Variation of Concentration of HCl Activators. (LTA Zeolite Difractogram Pattern Standard ICDD No.00-031-1261).

**Figure description:**
A = LTA Zeolite
Ca= Calcium Aluminum Silicate
M= Mulltite ($Al_{2,34}O_{4,83}Si_{0,66}$)
Q= *Quartz*

The effect of dealumination events and the increase in the Si/Al ratio in LTA zeolite can reduce the percent crystallinity of the zeolite. Dealumination is a process of releasing alumina from the main framework of the zeolite due to reacting with HCl which causes the Si/Al ratio to increase so that it can increase the acidity of the zeolite (formation of Bronsted acid and Lewis acid which are the active sites of acid in zeolite) and causes the silica structure in the main framework of the zeolite to become more reactive with $H^+$ ions and forms silanol bonds (Si-OH) due to hydrolysis of $H^+$ ions which increases during activation. Si-OH structure is also known as amorphous silica because it has a random and irregular arrangement of atoms and molecules, and is reactive towards $H^+$ (Mujiyanti et al., 2021) so that it is easy to polymerize and to dehydroxylate the separation of OH group and to form a siloxane bond, siloxane bond O-Si-O-Si-O which is a strong bond and causes the crystal structure to become silica gel. Silica gel is a form of irregular/amorphous component structure and therefore the crystallinity of Zeolite A is reduced (Cakicioglu-Ozkan & Ulku, 2005). Thus, the crystalline silica in the zeolite can be hydrolyzed and cause de-crystallization of the previously formed crystals A. Here is the moment when Silica Crystals are part of Zeolite A which is reactive when the Silica molar content increases. Figure 3 shows the equation of $Na_2(SiO_4)$ reacting with HCl to form $Si(OH)_4$. Meanwhile, Figure 4 shows the reaction equation for the formation of polymersilica (Mujiyanti et al., 2021).

The decrease in crystallinity is also caused by the increase in the Si/Al ratio which also causes a further nucleation process so that it undergoes rearrangement of the cations and changes the structure of A crystals to an amorphous form, thus allowing a decrease in the crystallinity value (Smaihi et al., 2003). Where in Table 3, LTA zeolite with 20% w/w activation was able to increase the highest percent crystallinity value of zeolite A, which was 68.25% wt after activation treatment to remove metal impurities and increase crystal purity of zeolite A. This has also been proven by the appearance of diffraction patterns zeolite A which are more abundant and sharper in intensity; and fewer Calcium Alluminate Silicate, Mullite, and Quartz

crystals appeared compared to the other three LTA zeolites.

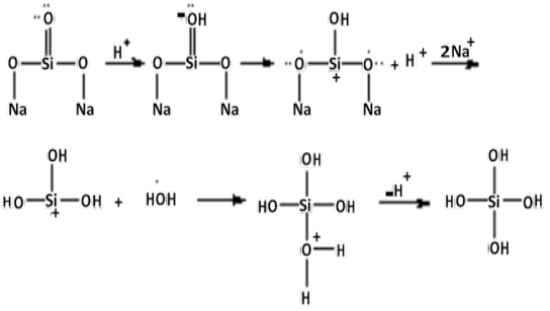

**Figure 3.** Reaction of $Si(OH)_4$ Formation.

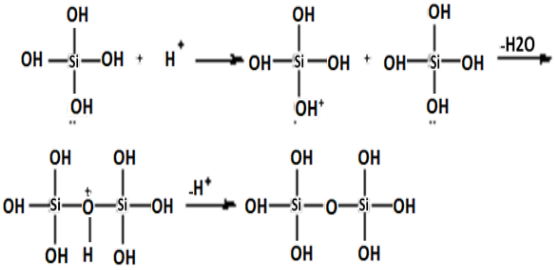

**Figure 4.** Polymersilica Process.

### 3.3. FTIR Analysis

The FTIR characterization of the LTA zeolite synthesis was carried out by looking at the absorption band at specific wave numbers in the range of 1250 – 300 $cm^{-1}$ which is shown in Figure 5, that is: in the range of 950 – 1250 $cm^{-1}$ it shows that the internal structure of the O-T-O tetrahedral is caused by asymmetric strain vibrations in the sample. The presence of an absorption band at wave number 420 - 500 $cm^{-1}$ is a bending vibration of the Si-O/Al-O bond which indicates that the 4R and 6R rings have formed as a result of the bending between the T-O-T bonds. In addition, there is another valley that shows the characteristics of zeolite A, namely at wave numbers of 500 – 650 $cm^{-1}$ which is a double ring vibration range indicating that *cages* have been formed as the *Secondary Building Units* (SBU) of zeolite A. The external vibrations of the double rings D4R or D6R are vibrations that characterize the structure formation of zeolite A(Xu et al., 2010). Finally, there is an absorption band at wave numbers between 300 - 400 $cm^{-1}$ indicating the formation of pore openings in the arrangement of zeolite cages (Alshameri et al., 2014).

Meanwhile, in the FTIR spectra of LTA zeolite with 20% w/w activation, there is an absorption band that shows a sharp bend with high intensity at a wave number of 565.21 $cm^{-1}$. This absorption indicates the formation of double rings D4R or D6R, denoting that zeolite crystals are formed in the gel matrix(Tong et al., 2014) (Tong et al., 2014) where the curves are sharper than the previous three zeolites in the wave range of 550 – 600 $cm^{-1}$. This shows that at the concentration of this activator, the degree of polymerization of tetrahedral SiO4 increased the largest compared to the results of the addition of activation at concentrations of 10% w/w, 15% w/w, and zeolite before activation. So that there was an increase in the emergence of seeds from LTA zeolite, due to the presence of sodium aluminasilica (Tong, et. Al., 2014).
The formation of absorption bands in the wavelength range of 300 - 400 $cm^{-1}$ on LTA zeolite activation at 10% w/w, 15% w/w and 20% w/w indicates that the surface has open pores. This absorption band shows the increasing concentration of peak activators produced sharper with higher intensity so that the zeolite pores will open even larger. This is because the more concentration given for activation, the more the presence of empty pores caused by the more impurities removed in the zeolite (Reyes et al., 2010).

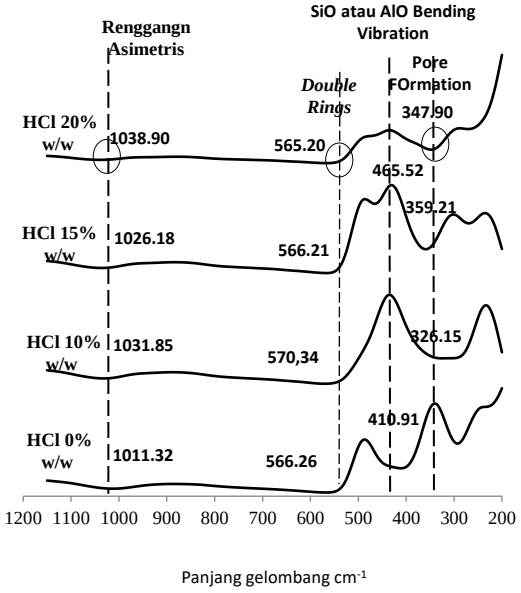


**Figure 5.** Results of FTIR Analysis on LTA Zeolite with Variations in HCl Concentration.

### 3.4. Morphology of LTA Zeolite

The results of the SEM analysis were the morphology images of activated LTA Zeolite on 10% w/w (Zeolite A-10), 15% w/w (Zeolite A-15) and 20% w/w (Zeolite A-20) with magnifications of 1000x, 5000x, 10,000x, and 20,000x.

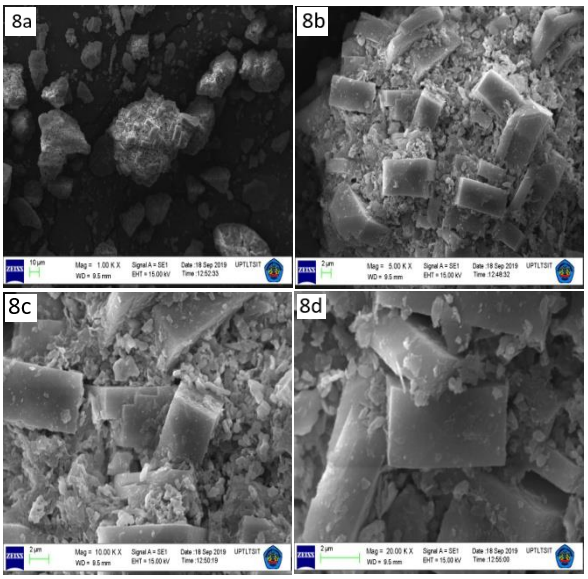


**Figure 8.** SEM results of Zeolite A-10 with 1000x (8a), 5000x (8b), 10,000x (8c), and 20,000x (8d) magnifications.

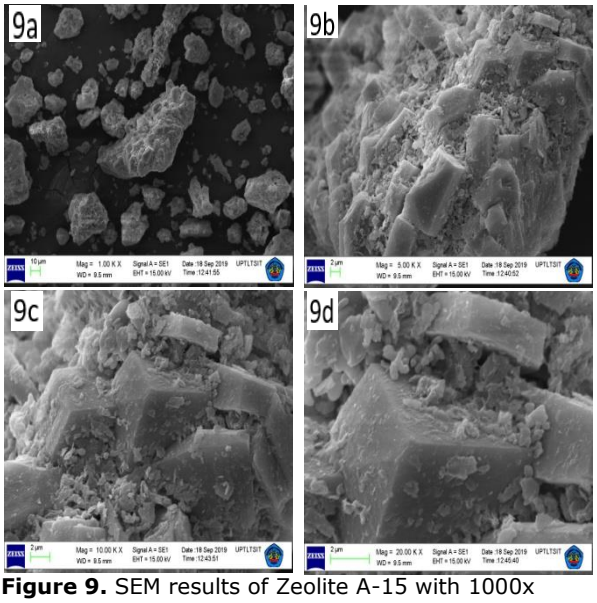


**Figure 9.** SEM results of Zeolite A-15 with 1000x (9a), 5000x (9b), 10,000x (9c), and 20,000x (9d) magnifications.

Figure 8 and Figure 9 showed that the LTA zeolite with activation levels of 10% w/w and 15% w/w, most of the products formed had identical morphological structures which are amorphous and very few formed into crystal shapes. As the concentration of HCl was increased by 20% w/w, it is shown in Figure 10 that most of the products are formed into crystals with a more cubical shapes, as well as the presence of smaller irregular granules compared to the two previous zeolites. This indicates that the 20% w/w increase of HCl concentration is the optimal concentration to remove metal impurities without causing the crystals to change shape to amorphous so as to increase the percent crystallinity of LTA zeolite (Paquin et al., 2015).

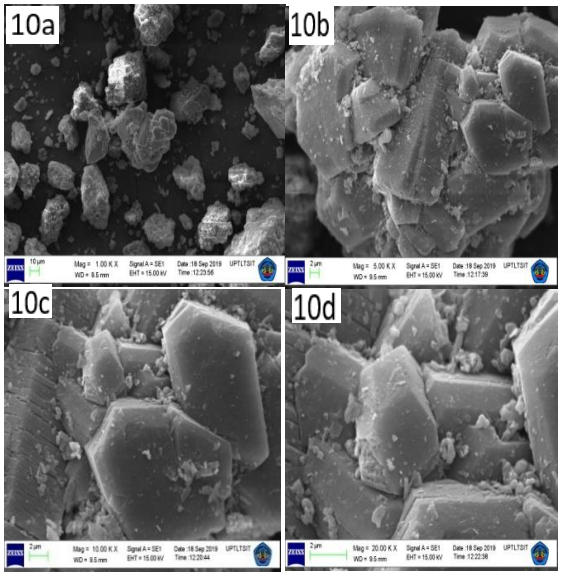


**Figure 10.** SEM results of Zeolite A-20 with 1000x (10a), 5000x (10b), 10,000x (10c), and 20,000x (10d) magnifications.

### 3.5. Adsorption Test Result

In this study, an adsorption test was carried out on water in ethanol. The results of synthetic LTA zeolite adsorption on water in ethanol are shown in Table 4. It is shows that the LTA zeolite with the largest water absorption was produced at a concentration of 20% w/w at an equilibrium time of 45 minutes to 50 minutes, the final concentration of ethanol was constant at 99.74% (v/v).

After reaching the equilibrium time, the difference in the water concentration in the adsorbent solution and surface has reached equilibrium, so the mass transfer process does not occur anymore. This is because the cavities and pores of the zeolite are completely filled with water, placing it in the state of saturated and reaching equilibrium.

**Table 4.** Adsorption Test Results.

| Zeolite A Variations in HCl Levels | Ethanol Level % (v/v) | Water Absorption % (v/v) |
|---|---|---|
| 0% w/w | 99.65 | 92.79 |
| 10% w/w | 97.65 | 51.94 |
| 15% w/w | 97.83 | 55.78 |
| 20% w/w | 99.74 | 94.78 |

With a final ethanol concentration of 99.74% (v/v) it can be said that the LTA zeolite can absorb water from the ethanol-water mixture

so that it can be used as FGE (Fuel Grade Ethanol) (Sekulić et al., 2014).

Table 4 shows that the LTA zeolite with the largest water absorption was produced at a concentration of 20% w/w at an equilibrium time of 45 minutes to 50 minutes, the final concentration of ethanol was constant at 99.74% (v/v). After reaching the equilibrium time, the difference in the water concentration in the adsorbent solution and surface has reached equilibrium, so the mass transfer process does not occur anymore. This is because the cavities and pores of the zeolite are completely filled with water, placing it in the state of saturated and reaching equilibrium. With a final ethanol concentration of 99.74% (v/v) it can be said that the LTA zeolite can absorb water from the ethanol-water mixture so that it can be used as FGE (Fuel Grade Ethanol) (Sekulić et al., 2014).

### 3.5.1. Adsorption Isotherm Model

Determining the adsorption isotherm model and adsorption capacity by ethanol-water adsorption test with 5 different ethanol-water concentrations until equilibrium time (50 minutes), the best adsorbent of LTA zeolite was 20% w/w of HCl concentration.

**Table 5.** Calculation of $q_e$ Value.

| Mixture of Ethanol – Water (% v/v) | $C_o$ (g/ml) | $C_e$ (g/ml) | $q_e$ (mg/g) |
|---|---|---|---|
| 70 – 30 | 0.300 | 0.145 | 0.775 |
| 80 – 20 | 0.200 | 0.050 | 0.749 |
| 85 – 15 | 0.150 | 0.041 | 0.545 |
| 90 – 10 | 0.100 | 0.011 | 0.445 |
| 95.1 – 4.9 | 0.049 | 0.003 | 0.232 |

$q_e$ = Amount of adsorbed substance per gram of adsorbent at equilibrium (mg/g).
Co = Initial concentration of solution (gr/ml).
Ce = Concentration of solution at equilibrium (gr/ml).

The following are Figures 11 and 12 showing the experimental data for the adsorption isotherm. The experimental data of the adsorption isotherm were analyzed using two models of adsorption isotherm, namely the Langmuir and Freundlich models. Langmuir isotherm is based on monolayer adsorption on the active side of a homogeneous adsorbent, whereas the Freundlich isotherm type assumes that the adsorbent has a heterogeneous surface and each molecule has different absorption potential (Setyaningsih & Hery Haerudin, 2009).

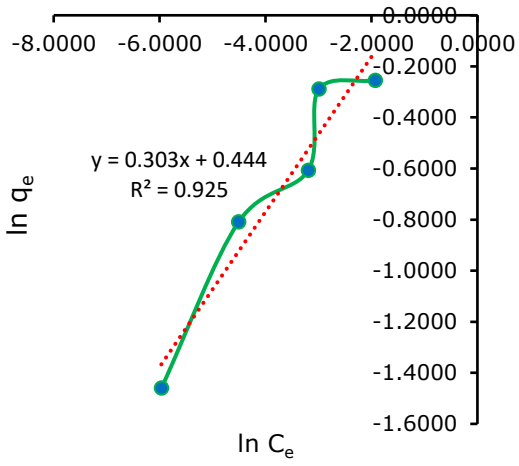


**Figure 11.** Freundlich Isotherm Linearization.

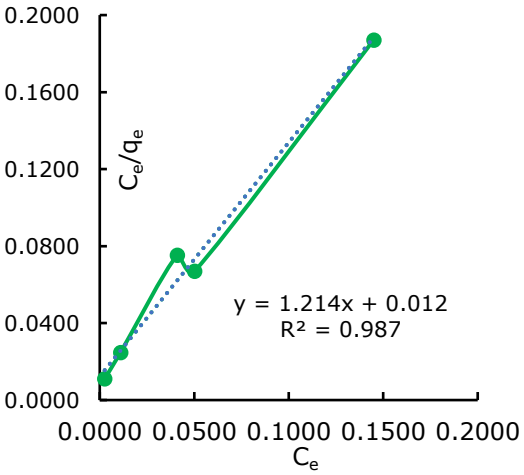


**Figure 12.** Langmuir Isotherm Linearization.

Based on Figure 12, it shows that the adsorption process follows the Langmuir isotherm adsorption model, with an $R^2$ value that is close to 1, which is 0.987. This is determined based on the value of $R^2$, where the value of $R^2$ which is closer to 1 indicates that the equation will follow the adsorption isotherm model (Tonu Lema et al., 2022). The Langmuir isotherm model shows that in the presence of an adsorption monolayer, the adsorbate on the surface of the adsorbent (zeolite) has a limited specific area (site), where once the adsorption site is occupied, further adsorption cannot occur in that area. Theoretically, further absorption cannot occur again, if saturation is reached (Saeed et al., 2009).

**Table 6.** Comparison of relationship coefficient value ($R^2$), adsorption capacity value, and adsorption intensity.

| Isotherm Model | $R^2$ | Adsorption Intensity (Ka/Kf) | Adsorption Capacity Rate ($q_m/n$) |
|---|---|---|---|
| Langmuir Isotherm | 0.987 | 0.01 | 83.33mg/g |
| Freundlich Isotherm | 0.925 | 1.56 | 3.30mg/g |

### 3.5.2. Adsoption Kinetics

Based on Table 7, it can be explained that zero-order kinetics means that the concentration of species does not affect the reaction rate, while first, second, and third-order kinetics means that the concentration of species affects the reaction rate. Ethanol-water adsorption by LTA zeolite follows a kinetic model of the order which has an $R^2$ value close to 1, following a graph plot seen from the correct linearization model and comparing the value of $q_e$ (theoretical) which is close to the value of $q_e$ (experimental). From the graph plot of the zeolite adsorption kinetics, it shows that the first and second order adsorption kinetics follow the correct linearization model, where for the first order the linearization graph tends to decrease while for the second order it tends to increase. Meanwhile, the zero order and third order do not follow the rules of the linearization model, where the zero order graph should be stable and flat and for the third order it should increase (Tonu Lema et al., 2022).

**Table 7.** Correlation coefficient value ($R^2$), reaction rate constant and $q_e$ value

| Parameter | Zero Order | First Order | Second Order | Third Order |
|---|---|---|---|---|
| $R^2$ | 0.878 | 0.116 | 0.953 | 0.214 |
| k g/( min-mg) | 0.004 | 0.039 | 0.436 | 0.538 |
| $q_e$ (exp) mg/g | | 0.232 | | |
| $q_e$(theoretical) mg/g | 0.432 | 0.006 | 0.289 | -0.169 |

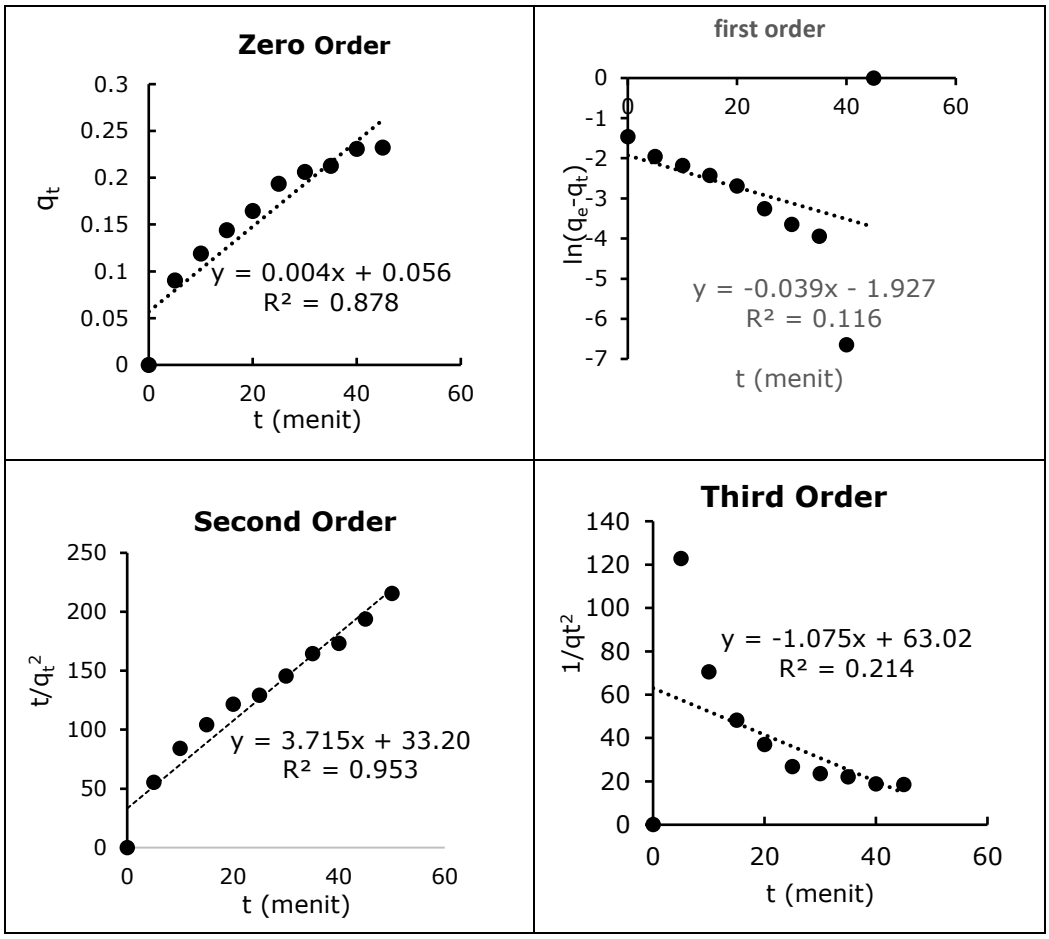


**Figure 13.** Zero, 1st , 2nd and 3rd order adsorption kinetics.

It can be concluded that the ethanol-water adsorption by LTA zeolite at a concentration of 20% w/w follows a second-order kinetic model which has an $R^2$ value closer to 1 than the other orders of 0.953 and a reaction rate constant of 0.436 g/w. (min-mg). The second order is a reaction that has an adsorption rate that is directly proportional to the concentration of its two followers or one squared follower (Heraldy et al., 2010).

## 4. Conclusion

The best result of this experimental is HCl concentration is at 20% w/w : Based on the XRD analysis, the highest percentage of crystallinity was obtained 68.25%, LTA zeolite content where the activator content of 20% w/w was able to remove metal impurities, did not cause dealumination and did not increase the ratio level of molar Si/Al which can change the crystal structure to be more amorphous so that the percentage of crystallinity can increase. The water adsorption isotherm pattern followed the Langmuir isotherm model with $R^2$ = 0.987, adsorption capacity qm = 83.33 mg water/g, adsorbent and adsorption intensity Ka = 0.01. The water adsorption kinetics by synthetic LTA zeolite with activator concentration were of 20% w/w according to pseudo second order adsorption kinetics model with the reaction rate constant of 0.436 g/(min-mg) and qe of 0.289 mg water/g adsorbent with the highest ethanol purity after 20% w/w activation of 99.74 v/v. So in this study, LTA zeolite from LNZ was successfully increased the surface area characteristics of zeolite without changing the crystal structure to amorphous by 33.01 $m^2/g$ after activation by 20% w/w of HCl concentration and obtained the highest ethanol purity which increased by 99.74% v/ v.

## Reference

Alshameri, A., Ibrahim, A., Assabri, A. M., Lei, X., Wang, H., & Yan, C. (2014). The Investigation into the Ammonium Removal Performance of Yemeni Natural Zeolite: Modification, Ion Exchange Mechanism, and Thermodynamics. Powder Technol. *258*, 20–31. https://doi.org/10.1016/j.powtec.2014.02.063

Bulut, E., Özacar, M., & Şengil, I. A. (2008). Adsorption of Malachite Green onto Bentonite: Equilibrium and Kinetic Studies and Process Design. Micropor. Mesopor. Mat. *115*(3), 234–246. https://doi.org/10.1016/j.micromeso.2008.01.039

Cakicioglu-Ozkan, F., & Ulku, S. (2005). The Effect of HCl Treatment on Water Vapor Adsorption Characteristics of Clinoptilolite Rich Natural Zeolite. Micropor. Mesopor. Mat.*77*(1), 47–53. https://doi.org/10.1016/j.micromeso.2004.08.013

Darmansyah, Simparmin, B. G., Dery, W., dan Hens, S. (2013). Synthesis of Lynde Type-A Zeolite (LTA) From Lampung Natural Zeolite (ZAL) Using Step Change Temperature Of Hydrothermal Method With SiO2/Al2O3 Variation Applied For Ethanol Dehydration. J. Chem. Process Eng. 4(1), 31–44

Ferella, F., Leone, S., Innocenzi, V., De Michelis, I., Taglieri, G., & Gallucci, K. (2019). Synthesis of Zeolites from Spent Fluid Catalytic Cracking Catalyst. J. Clean. Prod. *230*, 910–926. https://doi.org/10.1016/j.jclepro.2019.05.175

Ginting, S., Sari, D. P., Iryani, D. A., Darmansyah, D., Hanif, M., & Wardono, H. (2019). Synthesis of Lynde Type-A Zeolite (LTA) From Lampung Natural Zeolite (ZAL) Using Step Change Temperature Of Hydrothermal Method With SiO2/Al2O3 Variation Applied For Ethanol Dehydration. J. Chem. Process Eng. 4(1), 31–44 https://doi.org/10.33536/jcpe.v4i1.324

Heraldy, E., SW, H., & Sulistiyono, S. (2010). Characterization and Activation of Natural Zeolit From Ponorogo. Indones. J. Chemis. 3(2), 91–97. https://doi.org/10.22146/ijc.21891

Mirfendereski, M., & Mohammadi, T. (2016). Effects of Synthesis Parameters on the Characteristics of Naa Type Zeolite Nanoparticles. World Congress on Recent Advances in Nanotechnology, 1–8. https://doi.org/10.11159/icnnfc16.113

Mujiyanti, D. R., Ariyani, D., & Lisa, M. (2021). Silica Content Analysis of Siam Unus Rice Husk from South Kalimantan. Indones. J. Chem. Res. 9(2), 129–136. https://doi.org/10.30598//ijcr.2021.9-muj

Neolaka, Y. A. B., Lawa, Y., Naat, J., Riwu, A. A. P., Mango, A. W., Darmokoesoemo, H., Widyaningrum, B. A., Iqbal, M., & Kusuma, H. S. (2022). Efficiency of Activated Natural Zeolite-Based Magnetic Composite (ANZ-Fe3O4) as a Novel Adsorbent for Removal of Cr(VI) from Wastewater. J. Mater. Res. Technol. *18*, 2896–2909. https://doi.org/10.1016/j.jmrt.2022.03.153

Panitchakarn, P., Laosiripojana, N., Viriya-umpikul, N., & Pavasant, P. (2014). Synthesis of High-Purity Na-A and Na-X Zeolite from Coal Fly Ash. Journal of the Air and Waste Management Association, *64*(5), 586–596. https://doi.org/10.1080/10962247.2013.859184

Paquin, F., Rivnay, J., Salleo, A., Stingelin, N., & Silva, C. (2015). Multi-Phase Semicrystalline Microstructures Drive Exciton Dissociation in Neat Plastic Semiconductors. J. Mater. Chem. C, *3*, 10715–10722. https://doi.org/10.1039/b000000x

Ranjbar, Z. (2012). *Ethanol Dehydration With Protein Extracted Canola Meal in a Pressure Swing Adsorption Process*.

Reyes, C. A. R., Williams, C. D., & Alarcón, O. M. C. (2010). Synthesis of Zeolite LTA from Thermally Treated Kaolinite | Síntesis de Zeolita LTA a Partir de Caolinita Tratada Térmicamente. Rev. Fac. Ing. 53, 30–41.

Saeed, A., Iqbal, M., & Höll, W. H. (2009). Kinetics, Equilibrium and Mechanism of Cd2+ Removal from Aqueous Solution by Mungbean Husk. Journal of Hazardous Materials, 168(2–3), 1467–1475. https://doi.org/10.1016/j.jhazmat.2009.03.062

Sekulić, Ž., Kolonja, B., Kragović, M., Ivošević, B., & Mihajlović, S. (2014). Jakość Zeolitów Jako Funkcja Ich Uziarnienia. Gospodarka Surowcami Mineralnymi / Mineral Resources Management, *30*(3), 5–16. https://doi.org/10.2478/gospo-2014-0028

Setyaningsih, D., & Hery Haerudin, dan. (2009). Modification of Natural Zeolite as Molecular Sieve Material in Bioethanol Dehydration Process. J. Indones. Zeolite 8(2), 97–105.

Smaihi, M., Barida, O., & Valtchev, V. (2003). Investigation of the Crystallization Stages of LTA-Type Zeolite by Complementary Characterization Techniques. Eur. J. Inorg. Chem, *24*, 4370–4377. https://doi.org/10.1002/ejic.200300154

Tong, F., Ji, W., Li, M., Zeng, C., & Zhang, L. (2014). Investigation of the Crystallization of Zeolite A from Hydrogels Aged under High Pressure. CrystEngComm, *16*(36), 8563–8569. https://doi.org/10.1039/c4ce00688g

Tonu Lema, A., Sabuna, C., & Balu, Y. W. (2022). Optimization and Kinetic Study of Ende-Natural Zeolite as Candidates of Ammonia Adsorbent on Broiler Chicken Litter. KOVALEN: J. Riset Kimia, *8*(2), 150–157. https://doi.org/10.22487/kovalen.2022.v8.i2.15914

Triantafillidis, C. S., & Evmiridis, N. P. (2000). Dealuminated H-Y Zeolites: Influence of the Number and Type of Acid Sites on the Catalytic Activity for Isopropanol Dehydration. Ind. Eng. Chem. Res. *39*(9), 3233–3240. https://doi.org/10.1021/ie000002s

Wang, X., Ozdemir, O., Hampton, M. A., Nguyen, A. V., & Do, D. D. (2012). The Effect of Zeolite Treatment by Acids on Sodium Adsorption Ratio of Coal Seam Gas Water. Wat.Res. *46*(16), 5247–5254. https://doi.org/10.1016/j.watres.2012.07.006

Wardono, H., Ginting, S. B., & Sinulingga, E. A. (2018). The Use of Adsorbents of Lampung Natural Eolites/Coal-Fly Ash in Reducing Fuel Consumption and Exhaust Gas Emissions of a 4-Stroke Petrol Motorcycle. AIP Conf. Proc. *1977*(2018). https://doi.org/10.1063/1.5042916

Xu, R., Pang, W., Yu, J., Huo, Q., & Chen, J. (2010). Chemistry of Zeolites and Related Porous Materials: Synthesis and Structure. Chemistry of Zeolites and Related Porous Materials: Synthesis and Structure. https://doi.org/10.1002/9780470822371

Jurnal Rekayasa Kimia dan Lingkungan
(Journal of Chemical Engineering and Environment)
Volume 17, Number 2, Page 152 – 162, July - December, 2022
ISSN 1412-5064, e-ISSN 2356-1661
https://doi.org/10.23955/rkl.v17i2.26692